Analysis of experimental feasibility of polar-molecule-based phase gates

Elena Kuznetsova,[1,2] Robin Côté,[1] Kate Kirby,[2] and S. F. Yelin[1,2]
[1]*Department of Physics, University of Connecticut, Storrs, Connecticut 06269, USA*
[2]*ITAMP, Harvard-Smithsonian Center for Astrophysics, 60 Garden Street, Cambridge, Massachusetts 02138, USA*
(Received 24 September 2007; revised manuscript received 7 February 2008; published 9 July 2008)

We analyze a recently proposed physical implementation of a quantum computer based on polar molecules with "switchable" dipoles, i.e., dipole moments that can be switched "on" and "off". Conditional dipole-dipole interaction is an efficient tool for realizing two-qubit quantum gates necessary to construct universal gates. A set of general requirements for a molecular system is presented, which would provide an optimal combination of quantum gate times, coherence times, number of operations, high gate accuracy, and experimental feasibility. We proceed with an analysis of a two-qubit phase gate realization based on switchable dipole-dipole interactions between polar molecules in an optical lattice architecture. We consider one of the schemes proposed in our previous work [Phys. Rev. A **74**, 050301(R) (2006)], using specific molecules, such as CO and NF. We suggest suitable electronic states and transitions, and investigate requirements for the laser pulses driving them. Finally, we analyze possible sources of decoherence and list practical difficulties of the scheme.

DOI: 10.1103/PhysRevA.78.012313 PACS number(s): 03.67.Lx, 03.67.Mn

I. INTRODUCTION

Information processing relying on quantum mechanical rather than classical systems holds the promise for a dramatic speedup of such operations as factoring large numbers, searches of unstructured databases, and simulation of the dynamics of quantum mechanical systems [1]. Communication devices using optical fields with single photons would provide a level of security impossible with classical communication techniques [2]. Recent years have witnessed remarkable advances in both the theoretical and experimental development of quantum computing technologies, including demonstrations of basic building blocks necessary for quantum computing and quantum networking. Various approaches have been explored, including those based on trapped ions and neutral atoms [3,4], cavity QED [5], liquid NMR [6], and solid-state systems [7]. Recently, dipolar molecules were proposed as a system with characteristics optimal for physical implementation of quantum computing schemes [8]. Polar molecules combine the advantages of neutral atoms and ions (such as long coherence times, rich level structure, strong optical and microwave transitions, and well-developed techniques of coherent manipulation with optical and microwave pulses) and of quantum dots and superconducting circuits (easy control with electrostatic fields). Polar molecules are thus compatible with various architectures, including optical lattices, microwave, static and ac electric and magnetic traps and solid-state systems. An important aspect of these systems is the existence of electronic states which exhibit a large permanent dipole moment. The molecules can then be used for fast conditional dipole-dipole interactions resulting in two-qubit operations, necessary for construction of a universal set of qubit gates.

A number of specific implementations of quantum computing schemes with polar molecules have been suggested [8–15]. Recently we proposed a model of controllable dipole-dipole interaction between polar molecules [14], allowing one to implement a universal two-qubit gate, such as a phase gate. In this scheme, the state used to store a qubit and the additional state to turn the interaction "on" and "off" have permanent dipole moments of significantly different magnitude. The turning on and off mechanism can be called "switching" of the interaction, and the additional state used to perform it can be called a "switch" state. Ideally, one of the states has a zero moment, while the other one has a large dipole moment of several Debye, so that two molecules in this state will exhibit strong dipole-dipole interaction and acquire a π phase shift. Provided that the molecules can be excited only from one of the qubit states, for example, $|1\rangle$, only the $|11\rangle$ state of the two-qubit system will acquire a phase, resulting in a phase gate. In this approach only two selected molecules interact, which greatly simplifies the two-qubit gate compared to the case when all molecules interact at the same time.

Three realizations of the phase gate with polar molecules were proposed in our previous work [14]. Here we focus on one of these: the direct phase gate. It uses the molecular ground electronic state with a zero permanent dipole moment to store a qubit. To perform the gate operation, the molecules are then excited to an electronic state with a large dipole moment [see Fig. 1]. The scheme, utilizing electronic molecular transitions in the visible or uv range, can be most naturally implemented with cold molecules in optical lattices [3]. It can also be realized with molecules doped into solid-state matrices [16]. In the present work we analyze the ex-

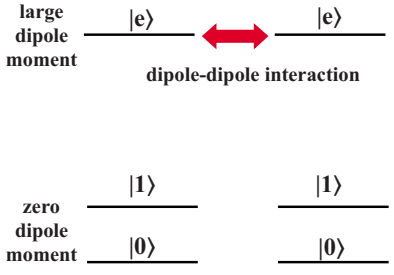

FIG. 1. (Color online) Schematic showing the direct variant of the phase gate based on controllable dipole-dipole interaction of polar molecules.

perimental feasibility of the proposed approach: identify candidate molecules, find an optimized realization of quantum gates (using the two-qubit phase gate as an example) resulting in small gate error, estimate parameters of gates, and analyze the sources of decoherence.

The organization of the paper is as follows. Section II presents a set of requirements which would provide the optimal performance for the implementation of quantum computing with polar molecules. In Sec. III we analyze the dipole-dipole interaction between two molecules and calculate the phase shift a two-qubit state acquires during the interaction time. We also analyze in detail the application of the dipole-blockade mechanism which would allow the gate operation to be independent of the distance between the interacting molecules and their relative orientation. In Sec. IV we investigate this direct dipole control scheme for the specific case of the CO molecule. Decoherence mechanisms are discussed in Sec. V, and our conclusions are presented in Sec. VI.

II. REQUIREMENTS FOR A POLAR MOLECULE QUBIT SYSTEM

In order to provide an optimal combination of long coherence times, short gate times (resulting in maximal number of operations), small gate errors, and experimental feasibility, a set of general requirements for a polar molecular system can be formulated.

(1) *Choice of qubit states*. Long-lived states are required to store a qubit. These should be well isolated from the environment, i.e., only weakly perturbed by electric and magnetic fields and various interactions, such as dipole-dipole, spin-spin, or black-body radiation. Good candidates are hyperfine and rotational states of a ground electronic molecular state having a negligible permanent dipole moment. To encode a qubit in hyperfine states, a ground electronic state with a nonzero electronic orbital and/or spin angular momentum is preferable in order to maximize the splitting between hyperfine sublevels.

(2) *Coupling strengths*. Fast one and two-qubit gates require the corresponding interaction strengths to be large. The storage states need long lifetimes. This means that the transition between the qubit states $|0\rangle$ and $|1\rangle$ should be forbidden and thus Raman transitions via an intermediate state could be used to perform one-qubit gates. An alternative approach is to map the qubit to some states coupled by a one-photon allowed transition. In both cases, the resulting transition coupling has to be strong. Choosing electric dipole-allowed transitions with dipole moments of a fraction of a Debye for one-qubit operations, and sufficiently large Rabi frequencies of the laser fields, one qubit gate times can be as short as femtosecond laser pulse durations.

(3) *Robust dipole-dipole interactions*. For an efficient phase gate, strong and robust dipole-dipole interactions are required. To maximize the strength of the interaction, one must choose the excited electronic state with a dipole moment as large as possible. Robustness of the interaction assumes that the phase error accumulated during the interaction time can be kept below an acceptable threshold value.

(4) *Cooling and trapping*. In order to fulfill the requirements of (1) and (3), a molecule has to be cooled down to sub-Kelvin temperatures (typical rotational transition frequencies ~ 10 GHz, giving the condition $T \ll 1$ K to avoid populating higher-energy rotational states) and trapped. To initialize qubits encoded in hyperfine sublevels with splittings of tens—hundreds kHz, molecules will have to be cooled to temperatures of the order of 100 nK to 1 μK [17]. Cooling to the translational ground state of an optical lattice potential is necessary to minimize decoherence.

(5) *Decoherence*. Provided that a qubit is encoded in hyperfine or rotational sublevels with typical lifetimes of the order of hours and typical optical lattice decoherence times on the order of seconds, the main decoherence mechanisms are (i) spontaneous emission of the electronically excited states; (ii) spatial dependence of the dipole-dipole interaction; and (iii) finite laser-linewidth and other light-induced decoherence. Excited electronic states with a life-time long compared to the gate time are necessary to minimize (i). Thus we need to consider metastable excited states, which do not couple to lower energy states by electric dipole- allowed transitions. Spatial dependence of the dipole-dipole interaction can result in undesirable excitation of high-energy translational states of the lattice potential. To avoid it, the interaction should be switched on and off adiabatically with respect to the potential oscillation frequency. Decoherence times stemming from finite laser linewidth of the order of ms are expected using phase-stabilized lasers [18].

III. CALCULATION OF THE PHASE AND MINIMIZATION OF PHASE ERROR

A. Dipole-dipole interaction strength

We consider the dependence of the accumulated phase on the separation and orientation of the molecular dipoles. We explore how the error per gate can be reduced below a threshold value at which fault-tolerant quantum computing can be realized. A typically cited desirable error threshold is 0.01%, while errors per gate demonstrated experimentally to date are $\sim 3\%$ [19]. Error-correction codes have therefore been developed that would allow fault-tolerant quantum computing with error per gate as high as 1% [20]. In our analysis we use the 1% threshold value, as an acceptable error tolerance.

We analyze the phase error assuming that two molecules, with positions $\boldsymbol{r}_1$ and $\boldsymbol{r}_2$ and intermolecular distance defined as $|\boldsymbol{R}|=|\boldsymbol{r}_2-\boldsymbol{r}_1|$ are in a state $|\Psi_{1,2}\rangle$, having a large dipole-dipole interaction matrix element $\langle\Psi_{1,2}|\hat{V}_{\text{dip-dip}}|\Psi_{1,2}\rangle \sim \langle\Psi_{1,2}|\hat{\boldsymbol{\mu}}_1\cdot\hat{\boldsymbol{\mu}}_2/|\boldsymbol{R}|^3|\Psi_{1,2}\rangle$. While the interaction is switched on a π phase shift accumulates. The state $|\Psi_{1,2}\rangle$ can be a product $|e_1\rangle|e_2\rangle \equiv |e_1e_2\rangle$ of the states of two molecules, each having a large dipole moment. This can be realized if $|e_i\rangle$ is a superposition of rotational states of a molecular electronic state produced by a dc electric field. It should be noted that a pure rotational state has a zero dipole moment in the laboratory frame, and it is the transition between J and $J\pm 1$ rotational states that manifests a dipole moment, which is called the permanent dipole moment of a molecule. Therefore, for a

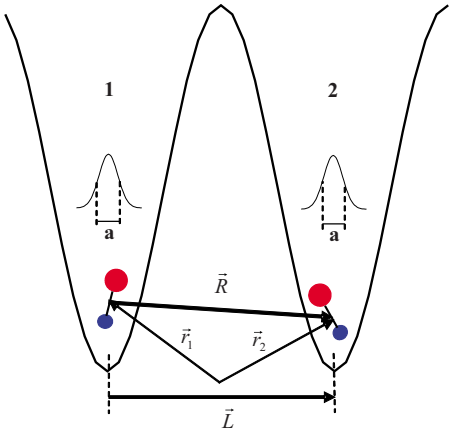

FIG. 2. (Color online) Definition of the relative position of two interacting molecules. The first and the second molecule are labeled 1 and 2, respectively.

state to have a nonzero dipole moment it should be mixed with other rotational states. Another possibility to have a nonzero dipole-dipole interaction matrix element $u \equiv \langle \hat{V}_{\text{dip-dip}} \rangle$ is to use an entangled state composed of two rotational states of interacting molecules, for example, $|\Psi_{1,2}\rangle = (|J_1=J, J_2=J+1\rangle \pm |J_1=J+1, J_2=J\rangle)/\sqrt{2}$, where we use the notation $|J_1, J_2\rangle$ with J_1, J_2 being rotational states of the first and second molecule, respectively. The entangled state is produced by the dipole-dipole interaction, mixing the initially degenerate $|J_1=J+1, J_2=J\rangle$ and $|J_1=J, J_2=J+1\rangle$ states, thus lifting the degeneracy. In the rest of the paper we will use a short notation $|\Psi_{1,2}\rangle = (|J, J+1\rangle \pm |J+1, J\rangle)/\sqrt{2}$ for the entangled state.

To analyze the phase dependence on the relative distance $|\boldsymbol{R}|$ and orientation of the dipole moments, we assume that each molecule is in a ground translational state $|g\rangle$ of a two-dimensional (2D) optical lattice potential. We also assume that molecules are confined in the third dimension. We therefore approximate the potential which each molecule experiences as an isotropic 3D harmonic potential. The phase accumulated during a period T is given by the expression $\phi = \langle \hat{\phi} \rangle = T \langle \Psi_{1,2}; g_1 g_2 | \hat{V}_{\text{dip-dip}} | \Psi_{1,2}; g_1 g_2 \rangle / \hbar$ in first order of perturbation theory. Here $|g_{1,2}\rangle$ are the translational ground states of molecules 1 and 2 in the lattice potential.

We can thus write

$$\phi = -\frac{T}{\hbar} \langle \Psi_{1,2}; g_1 g_2 | \left(\frac{\hat{\boldsymbol{\mu}}_1 \cdot \hat{\boldsymbol{\mu}}_2}{|\boldsymbol{R}|^3} - \frac{3(\hat{\boldsymbol{\mu}}_1 \cdot \boldsymbol{R})(\hat{\boldsymbol{\mu}}_2 \cdot \boldsymbol{R})}{|\boldsymbol{R}|^5} \right) \times |\Psi_{1,2}; g_1 g_2 \rangle. \quad (1)$$

In what follows we assume that the spatial extent of the translational ground-state wave function a is much less than the separation between molecules as shown in Fig. 2. In the Appendix we derive, in detail, an expression for the phase taking into account the deviation of $\boldsymbol{r}_1$ and $\boldsymbol{r}_2$ from the minimum of the lattice potential. Using a translational ground state wave function of the 3D isotropic harmonic potential, as shown in the Appendix, the matrix element (1) is obtained as

$$\phi \approx -\frac{T}{\hbar} \left\{ \frac{\boldsymbol{\mu}_1 \cdot \boldsymbol{\mu}_2}{L^3} \left[1 + \frac{15a^2}{L^2} + O\left(\frac{a^4}{L^4}\right) \right] - \frac{3(\boldsymbol{\mu}_1 \cdot \boldsymbol{L})(\boldsymbol{\mu}_2 \cdot \boldsymbol{L})}{L^5} \left[1 + \frac{35a^2}{L^2} + O\left(\frac{a^4}{L^4}\right) \right] \right\}, \quad (2)$$

where $\boldsymbol{L}$ denotes the vector connecting lattice potential minima, occupied by molecules 1 and 2 [see Fig. 2], and $L = |\boldsymbol{L}|$. In Eq. (2) we also performed averaging over the large dipole moment state $|\Psi_{1,2}\rangle$ and denoted average dipole moments as $\langle \hat{\boldsymbol{\mu}}_{1,2} \rangle \equiv \boldsymbol{\mu}_{1,2}$. In the case of $|\Psi_{1,2}\rangle = |e_1 e_2\rangle$ the corresponding matrix element is given by $\boldsymbol{\mu}_i = \langle e_i | \hat{\boldsymbol{\mu}}_i | e_i \rangle$; in the case of the entangled state $|\Psi_{1,2}\rangle = (|J, J+1\rangle \pm |J+1, J\rangle)/\sqrt{2}$, the first term in Eq. (2) is $\boldsymbol{\mu}_1 \cdot \boldsymbol{\mu}_2 = \pm \text{Re}(\boldsymbol{\mu}_{1J,J+1} \cdot \boldsymbol{\mu}^*_{2J,J+1})$ and the second one is $(\boldsymbol{\mu}_1 \cdot \boldsymbol{L})(\boldsymbol{\mu}_2 \cdot \boldsymbol{L}) = \pm [\text{Re}(\boldsymbol{\mu}_{1J,J+1} \cdot \boldsymbol{L}) \times (\boldsymbol{\mu}^*_{2J,J+1} \cdot \boldsymbol{L})]$, where $\boldsymbol{\mu}_{iJ,J+1} = \langle J, M | \hat{\boldsymbol{\mu}}_i | J+1, M' \rangle$.

For a simple estimate of the mean distance a molecule travels in the ground state of an optical lattice potential, we make a harmonic approximation of the potential $\Sigma_{i=1}^{3} V_0 \sin^2(kx_i) \approx V_0 k^2 \Sigma_i x_i^2$, with the frequency $\omega = k\sqrt{2V_0/m}$ and the corresponding translational ground-state wave function width $a = \sqrt{\hbar/m\omega}$. A typical potential depth experienced by a molecule in a lattice is $V_0 = \eta E_R = \eta \hbar^2 k^2 / 2m$, where m is the molecular mass, E_R is the molecular recoil energy and η is the dimensionless potential depth appropriate for a molecule ($\eta = 20$–100). The width a can be then related to the lattice field wavelength λ and the lattice depth η as $a = (2\eta)^{-1/4} \lambda / 2\pi$. For molecules in neighboring lattice sites $L = \lambda/2$, and the ratio $a/L \sim 0.1$, so that the terms $\sim O(a^4/L^4)$ can be neglected when the phase is calculated at the error per gate of 1% considered in this work.

The fidelity of the phase gate, which is directly related to a phase error during the gate operation, could possibly be affected by the uncertainty in the relative distance of the molecules, misalignment of their dipole moments, and the stability of the optical excitation pulses. Dipole-dipole interaction between molecules in the large dipole moment state can result in an energy shift and broadening of the molecular levels. While the shift is not important and can always be experimentally measured, leading to a rescaling of the energy levels, broadening will lead to uncertainty in the accumulated phase, and, therefore, to a phase error. To minimize the phase error, broadening has to be avoided.

First, we note that the $|\Psi_{1,2} g_1 g_2\rangle$ state is not an eigenstate of the total Hamiltonian, which is a sum of internal molecular electronic, vibrational, and rotational terms, plus translational and dipole-dipole interaction terms. The dipole-dipole interaction will admix higher-energy translational states of a lattice potential as well as higher-energy rotational states. However, if the molecules are transferred to the large dipole moment state adiabatically, i.e., slow enough with respect to a typical separation between the total Hamiltonian eigenenergies, the $|\Psi_{1,2} g_1 g_2\rangle$ state will adiabatically evolve into one of the eigenstates. Then the accumulated phase will be given by $\phi = \epsilon T / \hbar$, where ϵ is the corresponding eigenenergy. As we show in the Appendix, in this case the phase can be approximated by Eq. (2) with an acceptable error $<1\%$. Alternatively, the energy shift associated with the eigenstate

can be directly measured experimentally for any pair of molecules in the lattice, giving a precise value of ϵ. We conclude, therefore, that it is possible to realize the direct phase gate with an error per gate below a threshold value 1% set in this work, provided that the dipole-dipole interaction is switched on adiabatically.

We demonstrate in the Appendix that, for a typical polar molecule in an optical lattice, mixing of translational states due to dipole-dipole interaction will be small. This mixing will result in energy shifts of the translational states less than 1% of their unperturbed energy spacing. Similarly, mixing of rotational states, because of the larger energy splitting between adjacent rotational levels, will be even smaller. The separation of the eigenvalues of the total Hamiltonian is of the order of the translational energy spacing $\hbar\omega$. Thus, in the direct phase gate, adiabatic excitation requires that the duration of optical pulses transferring molecules from the qubit state $|1\rangle$ to the large dipole moment state $|\Psi_{1,2}g_1g_2\rangle$, be much larger that ω^{-1}. Nonadiabatic, fast transfer of molecules to the large dipole moment state $|\Psi_{1,2}g_1g_2\rangle$ will excite several eigenstates having contributions from higher translational states. Excitation of these states will result in a phase error $\sim a/L$, significantly exceeding the 1% threshold value.

In the case when the large dipole moment state is the entangled state, the orientation of the dipole moments is chosen by selection rules between different components of rotational states and therefore there is no uncertainty in the orientation of the dipoles and, thus, the accumulated phase. If the large dipole moment state is a tensorial product of dc electric field induced "pendular" states of each molecule, there is no uncertainty provided that the electric field is switched on adiabatically. In this case the system evolves into an eigenstate of the total Hamiltonian, including the $-\boldsymbol{\mu}\cdot\boldsymbol{E}$ term.

The phase gate operation time is the sum of the duration of the optical pulses exciting and deexciting the molecules, plus the period of time when the dipole-dipole interaction is switched on. This time will depend on the spatial separation between the two molecules, resulting in different gate times for each pair. Experimentally it can be cumbersome. To make the operation time independent of the molecular distance, and in general to make the gate more robust against all types of errors, a dipole blockade mechanism can be used, which we discuss below.

B. Dipole-blockade mechanism for the direct phase gate

The dipole blockade mechanism was introduced for quantum information processing with Rydberg atoms in Ref. [21]. A variant of the dipole blockade based on the strong van der Waals interactions between Rydberg atoms (vdW blockade) has been explored experimentally in Ref. [22]. The underlying principle is that because of the strong interaction between Rydberg atoms, the doubly excited states corresponding to the excitation of two atoms can be shifted out of resonance with the excitation laser, in effect blockading the transition of the second atom to the Rydberg level. Thus, one atom can be resonantly excited into a Rydberg state, but additional Rydberg excitations of neighboring atoms are prevented by the large energy shift.

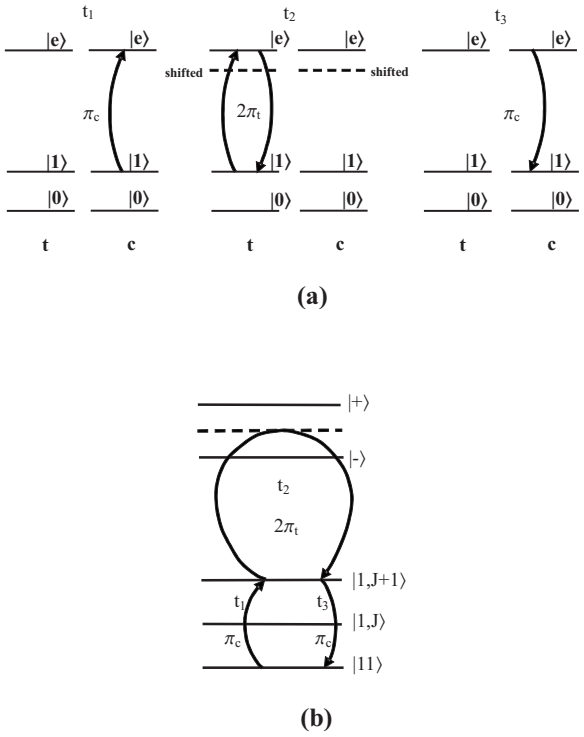

FIG. 3. Principles of the dipole blockade mechanism for the direct phase gate in the case of (a) the large dipole moment state $|\Psi_{1,2}\rangle=|e_1e_2\rangle$; (b) an entangled large dipole moment state $|\Psi_{1,2}\rangle=|\pm\rangle=(|J,J+1\rangle\pm|J+1,J\rangle)/\sqrt{2}$. The sequence of pulses applied to the control and target molecules is illustrated.

The same general idea can be applied to polar molecules. An important advantage of the dipole blockade mechanism is its insensitivity to the exact position of the interacting molecules, which makes the gate duration equal for all molecular qubits regardless of their relative separation. We will first describe how the dipole-blockade effect can be used for the direct phase gate assuming that $|\Psi_{1,2}\rangle=|e_1e_2\rangle$ and then show how it can be realized with $|\Psi_{1,2}\rangle\sim|J,J+1\rangle\pm|J+1,J\rangle$.

If the dipole-dipole interaction is strong enough so that $u\equiv\langle V_{\text{dip-dip}}\rangle$ is much larger than the bandwidth and the Rabi frequency of an excitation laser, the doubly excited state $|e_1e_2\rangle$ will be shifted out of resonance and never excited. If we denote one molecule as the control molecule (c), and the other as the target molecule (t), the state of the target molecule will depend on the state of the control, provided that the molecules can be addressed individually. The ability to drive a 2π transition on the target molecule therefore depends on whether the control molecule is excited (see Fig. 3). The phase gate is then implemented as shown in Fig. 3(a). At t_1 we apply a π_c pulse to the control (c) molecule and populate the state $|e_2\rangle$. At t_2 we apply a $2\pi_t$ pulse to the target molecule: if the control molecule is already in $|e_2\rangle$, the dipole-dipole interaction shifts the state $|e_1\rangle$ of the target molecule and the photon is off resonance, so the target molecule is not excited. During the $2\pi_t$ pulse the target molecule acquires a phase shift $\delta\phi=\pi\Omega_{2\pi}/u\ll\pi$ provided that $u\gg\Omega_{2\pi}$, where $\Omega_{2\pi}$ is the $2\pi_t$ pulse Rabi frequency. If the control molecule is not in $|e_2\rangle$ (i.e., it was in the $|0\rangle$ state before the first π_c pulse) the target molecule acquires a π

phase shift after the $2\pi_t$ pulse, since in this case the $|e_1\rangle$ state is not shifted and the pulse is resonant. Finally, at t_3 we deexcite the control molecule with another π_c pulse. The corresponding phase gate can be summarized as

$$\begin{aligned}
&|00\rangle \xrightarrow{\pi_c} |00\rangle \xrightarrow{2\pi_t} |00\rangle \xrightarrow{\pi_c} |00\rangle,\\
&|01\rangle \xrightarrow{\pi_c} i|0e\rangle \xrightarrow{2\pi_t} i|0e\rangle \xrightarrow{\pi_c} -|01\rangle,\\
&|10\rangle \xrightarrow{\pi_c} |10\rangle \xrightarrow{2\pi_t} -|10\rangle \xrightarrow{\pi_c} -|10\rangle,\\
&|11\rangle \xrightarrow{\pi_c} i|1e\rangle \xrightarrow{2\pi_t} ie^{i\delta\phi}|1e\rangle \xrightarrow{\pi_c} -e^{i\delta\phi}|11\rangle \qquad (3)
\end{aligned}$$

(here and throughout the paper the first state of a two-qubit state refers to the target and the second to the control molecule). This sequence of excitation pulses will entangle the two molecules. The dipole-dipole blockade interaction plays out as the suppressed change of $i|1e\rangle$ in the last line. If $u \gg \Omega_{2\pi}$, the residual phase $\delta\phi$ can be neglected. All states except $|00\rangle$ acquire a π phase, resulting in the phase gate.

We now analyze the dipole-blockade mechanism in the case when $|\Psi_{1,2}\rangle \sim |J,J+1\rangle \pm |J+1,J\rangle$. When the dipole moment of the $J \rightarrow J+1$ transition is large, the degeneracy of the states $|J,J+1\rangle$ and $|J+1,J\rangle$ is lifted by the dipole-dipole interaction and the states are strongly mixed, forming the eigenstates of the total Hamiltonian including the dipole-dipole interaction term

$$|\pm\rangle = (|J,J+1\rangle \pm |J+1,J\rangle)/\sqrt{2}. \qquad (4)$$

The $|\pm\rangle$ states are shifted in energy from the original degenerate $|J,J+1\rangle$, $|J+1,J\rangle$ states by $\pm u$, respectively. The dipole-blockade mechanism can now be implemented in the same way as before [see Fig. 3(b)]. First, a π_c pulse at t_1 excites a control molecule from the qubit state $|1\rangle$ into the $|J+1\rangle$ rotational state of the large dipole moment electronic state. Next, at t_2 a $2\pi_t$ pulse is applied to the target molecule, resonant with the unshifted $|1,J+1\rangle \rightarrow |J,J+1\rangle$ transition. It will then interact with both $|+\rangle$ and $|-\rangle$ states, which are shifted from resonance with the pulse due to the dipole-dipole interaction. If the shift is much larger than the Rabi frequency and the bandwidth of the $2\pi_t$ pulse, the pulse will be far-detuned from both states and the target molecule will not be excited. In this case the $2\pi_t$ pulse does not produce any phase shift of the two-qubit state due to destructive interference of transition probabilities from the $|1,J+1\rangle$ state into the $|+\rangle$ and $|-\rangle$ states, similar to the electromagnetically induced transparency effect [23]. If the control molecule is initially in the $|0\rangle$ state, i.e., it is not excited by the first π_c pulse, there is no dipole-dipole interaction and the $2\pi_t$ pulse applied to the target molecule is resonant with the $|1,0\rangle \rightarrow |J,0\rangle$ transition, causing a π phase shift. The phase gate in this case is described by the same Eq. (3).

Since the exact value of the dipole-dipole interaction strength and, therefore, the accumulated phase is not important if the dipole blockade mechanism is used, the gate operation time becomes independent of the molecular separation, resulting in a much simpler setup. In the next section, we describe the direct scheme using the CO molecule as an example.

IV. APPLICATION TO THE CO MOLECULE

Carbon monoxide (CO) has a small permanent dipole moment ($\sim 0.1D$) in the vibrational level $v=0$ of the ground electronic state $X\ ^1\Sigma^+$, which makes it suitable for our phase gate implementation. If we choose an isotopic variant of CO, the qubit can be encoded in hyperfine sublevels of the ground rovibrational state, weakly coupled with other states in the presence of static and nonresonant electromagnetic fields. An excited metastable $a\ ^3\Pi_0$ state of the CO molecule has a reasonably large permanent electric dipole moment of $\sim 1.37D$ [24]. As the large dipole moment state $|\Psi_{1,2}\rangle$ we can then in principle choose either a product state of large dipole moment states of two molecules or an entangled state. If we choose the product state, a dc electric field mixing rotational states has to be applied to induce a dipole moment in the $a\ ^3\Pi_0$ state of each molecule. We can estimate the magnitude of the field required to induce the dipole moment of the order of the permanent one as $\mathcal{E} \sim B\hbar/\mu \sim 10^5$ V/cm, where we use the rotational constant of the $a\ ^3\Pi_0$ state $B=1.69$ cm^{-1} and $\mu=1.37D$. This high electric field will lead to faster qubit decoherence, since the dipole moment of the storage $X\ ^1\Sigma^+$ state is not exactly zero. To minimize decoherence of the qubit storage state and to simplify the setup, an entangled electric field free superposition $|\Psi_{1,2}\rangle = (|J,J+1\rangle \pm |J+1,J\rangle)/\sqrt{2}$ can be used as the large dipole moment state. Since the phase gate with the CO molecule involves transitions in the uv range, an optical lattice architecture would be a natural choice for this setup. Ultracold CO molecules have not yet been produced experimentally, but techniques of cooling and trapping of neutral polar molecules are rapidly developing [17,25]. Translationally cold CO molecules (~ 1 K) are produced in a supersonic expansion of a molecular beam, and can be further decelerated in multiple stage pulsed electric fields. Velocities of CO molecules in a low-field seeking component of the metastable $a^3\Pi_1$ $J=1$ level from 225 to 98 m/s have been demonstrated in an array of 63 pulsed electric field stages [26]. By increasing the number of stages, the molecules can be brought to a standstill. There is also the possibility of slowing molecules essentially down to zero velocity using a far-detuned traveling optical lattice [27]. Once at a standstill the molecules can be transferred from the $a\ ^3\Pi_1$ $J=1$ to the ground $X\ ^1\Sigma^+$ high-field seeking $J=0$ state with an optical π pulse, and trapped in an ac electric [28] or optical trap [29]. The ground state $X\ ^1\Sigma^+$ has a small magnetic dipole moment originating from nuclear spins of isotopic C and O, and therefore is not a good candidate for magnetic trapping. For molecules in a high-field seeking state, further cooling to ultracold temperatures via evaporative cooling may be possible. We start with an analysis of the hyperfine structure of isotopic CO molecules in the $X\ ^1\Sigma^+$ and $a\ ^3\Pi_0$ states.

A. Hyperfine structure of CO

There are three stable CO isotopomers with at least one nucleus having a nonzero spin: ^{13}CO (1% abundance), C^{17}O

(0.038% abundance), and $^{13}C^{17}O$ (3.8×10^{-4}% abundance). The ^{13}C and ^{17}O nuclear spins are $I_C=1/2$ and $I_O=5/2$. For the ground rotational state $J=0$ of the $X\ ^1\Sigma^+$ electronic state the coupling with the nuclear spin is described by the Hamiltonian $H_{hfs}=b\boldsymbol{J}\cdot\boldsymbol{I}-eQqF_{Cas}(\boldsymbol{I},\boldsymbol{J})$, where $F_{Cas}(\boldsymbol{I},\boldsymbol{J})=[3C(C+1)/4-I(I+1)J(J+1)]/2I(2I-1)(2J-1)(2J+3)$ is the Casimir function [with $C=F(F+1)-I(I+1)-J(J+1)$] and $\boldsymbol{F}=\boldsymbol{J}+\boldsymbol{I}$. For $J=0$ ($F=I$), the coupling term vanishes, resulting in zero hyperfine splitting in the ground state for both ^{13}CO and $C^{17}O$. A small hyperfine splitting is present in $^{13}C^{17}O$ due to the interaction of the carbon and oxygen nuclear spins. The level structure of the lowest rotational states of the $X\ ^1\Sigma^+$ and $a\ ^3\Pi$ states is shown in Fig. 4 [30]. When Zeeman split by an external magnetic field, the $\pm1/2$ nuclear spin sublevels of ^{13}CO can be used as $|0\rangle$ and $|1\rangle$ qubit states, respectively. For the $|\Psi_{1,2}\rangle$ state, an entangled state of hyperfine substates of $J=0$ and $J=1$ rotational levels of the $a\ ^3\Pi_0$ states of two molecules can be chosen. For example, the states $|J=0,F=1/2,M=+1/2\rangle$ and $|J=1,F=3/2,M=+1/2\rangle$ of the interacting molecules can form the $|\pm\rangle$ large dipole moment entangled states [see Eq. (4)]. The corresponding dipole-dipole interaction matrix element for these states is $u=\langle\pm|\hat{\boldsymbol{\mu}}_1\hat{\boldsymbol{\mu}}_2/\hbar L^3|\pm\rangle=\pm4|\langle J=0,M=0|\mu_z|J=1,M=0\rangle|^2/3\hbar L^3=\pm4\mu^2/9\hbar L^3$. Taking $\mu=1.37$ D and two values of $L=\lambda/2$, e.g., $L=100$ and 500 nm, realizable with commercially available lasers, we obtain the dipole-dipole interaction strength $u\sim8.3\times10^5\ s^{-1}$ for these two L values (corresponding to $u/2\pi=130$ kHz and $u/2\pi=1.6$ kHz, respectively) for molecules in neighboring lattice sites. Rotational states of the metastable $a\ ^3\Pi_0$ state are split into two sublevels of opposite parity due to Λ doubling [31]. To meet the selection rule that only states of opposite parity are coupled by an electric-dipole allowed transition, we choose the $-$ component of the $J=1$ and the $+$ component of the $J=0$ states of $a\ ^3\Pi_0$ for our scheme. With this choice the $J=0-J=1$ transition in the metastable state is allowed as well as the transition between the $+$ parity $J=0$ ground rovibrational level of the $X\ ^1\Sigma^+$ state and the $-$ parity $J=1$ sublevel of the $a\ ^3\Pi_0$ state.

The Zeeman splitting in the ground electronic state is small, scaling as ~1 kHz/G, while in the excited state it scales as ~1 MHz/G due to the nonzero electronic angular momentum of the $a\ ^3\Pi_0$ state [32]. This means that magnetic fields of ~10 G will suffice to make the splitting of the Zeeman levels of the $a\ ^3\Pi$ rotational states resolvable and much larger than the dipole-dipole interaction induced splitting. Selective excitation of $|1\rangle$ can then be realized with a σ^+ laser pulse resonant with the $-1/2\rightarrow+1/2$ transition between the ground and excited electronic states as shown in Fig. 4(a). Single qubit rotations can be performed with far-detuned Raman pulses via sublevels of the $|J=1,F=1/2\rangle$ or $|J=1,F=3/2\rangle$ hyperfine states.

In the case of $^{13}C^{17}O$, the $M_F=2,3$ states of hyperfine sublevels $F_1=2,3$ of the ground rovibrational state can be utilized as the $|0\rangle$, $|1\rangle$ qubit states, respectively. For the $|\Psi_{1,2}\rangle$ state, the entangled state of $|J=1,F_1=4,M_{F1}=4\rangle$ and $|J=0,F_1=3,M_{F1}=3\rangle$ of the excited electronic state of the two interacting molecules can be used. Choosing the $F_1=4,M_{F1}=4$ component ensures that it is mixed with only one substate of the $J=0$ hyperfine manifold ($F_1=3,M_{F1}=3$),

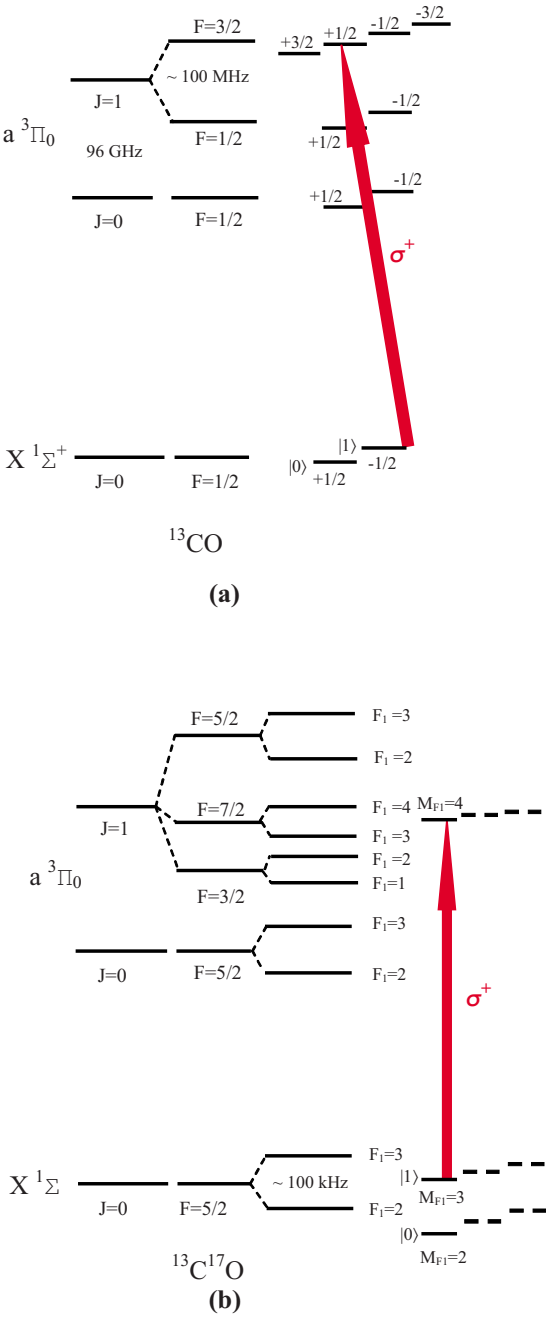

FIG. 4. (Color online) Hyperfine structure and Zeeman splittings of the lowest rotational states of the ground $X\ ^1\Sigma^+$ and excited $a\ ^3\Pi_0$ electronic states of two isotopomers of CO along with schemes of selective excitation of the $|1\rangle$ qubit state. (a) Illustrates the scheme with hyperfine levels for ^{13}CO and (b) illustrates the scheme for hyperfine levels appropriate for $^{13}C^{17}O$.

which simplifies the analysis. In this case the dipole-dipole interaction matrix elements are

$$u=\langle\pm|\hat{\boldsymbol{\mu}}_1\cdot\hat{\boldsymbol{\mu}}_2/\hbar L^3-3(\hat{\boldsymbol{\mu}}_1\cdot\boldsymbol{L})(\hat{\boldsymbol{\mu}}_2\cdot\boldsymbol{L})/\hbar L^5|\pm\rangle$$
$$=\mp4\sum_{i=x,y}|\langle J=0,M=0|\mu_i|J=1,M=1\rangle|^2/7\hbar L^3$$
$$=\mp4\mu^2/21\hbar L^3.$$

Taking the same μ and the range of L as previously, we obtain $u \sim (3.6\times 10^5 - 2\times 10^3)$ s^{-1} (60 kHz–300 Hz) for two molecules in neighboring lattice sites.

Hyperfine splittings of ~10–100 MHz are expected in the $a\ ^3\Pi$ state of $^{13}C^{17}O$ due to the strong electron-spin–nuclear-spin interaction, so that the hyperfine structure in this state is expected to be resolved with a narrow-band laser. Selective excitation of $|1\rangle$ can then be realized using a σ^+ polarized laser pulse resonant with the $|J=0,F=5/2,F_1=3,M_{F1}=3\rangle \rightarrow |J=1,F=7/2,F_1=4,M_{F1}=4\rangle$ transition, as shown in Fig. 4(b). Single qubit manipulation can also be performed via sublevels of this hyperfine state using polarized laser pulses.

B. Phase gate operation time

1. Phase gate without the dipole blockade

As we discussed in Sec. III, if both molecules are excited to the state $|\Psi_{1,2}g_1g_2\rangle$ slowly enough such that the dipole-dipole interaction is switched on adiabatically, the molecules are transferred into an eigenstate of the total Hamiltonian, and the accumulated phase can be calculated using Eq. (2). The phase gate in this case is straightforward: if both molecules are in the qubit state $|1\rangle$ they are simultaneously excited to the large dipole moment state $|\Psi_{1,2}g_1g_2\rangle$, experience the dipole-dipole interaction during an interaction time T, acquire a π phase shift and are, finally, deexcited. The phase gate is then described by the equation

$$
\begin{aligned}
&|00\rangle \overset{\pi}{\rightarrow} |00\rangle \rightarrow |00\rangle \overset{\pi}{\rightarrow} |00\rangle,\\
&|01\rangle \overset{\pi}{\rightarrow} i|0e\rangle \rightarrow i|0e\rangle \overset{\pi}{\rightarrow} -|01\rangle,\\
&|10\rangle \overset{\pi}{\rightarrow} i|e0\rangle \rightarrow i|e0\rangle \overset{\pi}{\rightarrow} -|10\rangle,\\
&|11\rangle \overset{\pi}{\rightarrow} -|ee\rangle \rightarrow |ee\rangle \overset{\pi}{\rightarrow} -|11\rangle,
\end{aligned}
\tag{5}
$$

where π denotes an optical π pulse transferring both molecules to the large dipole moment state.

We can estimate the gate operation time for the CO molecule. For ^{12}CO, choosing the $|\Psi_{1,2}\rangle$ as an entangled state of $|J=0,F=1/2,M=+1/2\rangle$ and $|J=1,F=3/2,M=+1/2\rangle$ sublevels of the a $^3\Pi_0$ state, the corresponding dipole-dipole interaction strength is in the range $u=4\mu^2/9\hbar L^3 \sim 10^4 - 8.3\times 10^5$ s^{-1} for values of the intermolecular separation $L=\lambda/2$ between 500 and 100 nm. The time T, required to accumulate the phase shift π, is therefore $T=\pi/u \sim 3.1\times 10^{-4} - 3.7\times 10^{-6}$ s, respectively. Adiabatic excitation of the large dipole moment state requires that the optical π pulses be much longer than ω^{-1}, where ω is the energy splitting of the motional states in the optical lattice. Taking $\omega \sim 100$ kHz and the pulse duration T_π an order of magnitude larger than ω^{-1}, we can estimate the total gate operation time as $T_{\text{gate}}=2T_\pi+T \sim 3.4\times 10^{-4} - 3.6\times 10^{-5}$ s. For $^{13}C^{17}O$ choosing the $|\Psi_{1,2}\rangle$ as an entangled state of the $|J=1,F_1=4,M_{F1}=4\rangle$ and $|J=0,F_1=3,M_{F1}=3\rangle$ sublevels of the a $^3\Pi_0$ state, the dipole-dipole interaction strength is $u=4\mu^2/21\hbar L^3 \sim 2\times 10^3 - 3.6\times 10^5$ s^{-1}. In this case, the π phase shift accumulation time is $T=\pi/u \sim 1.6\times 10^{-3} - 8.7\times 10^{-6}$ s. Assuming the same duration of optical π pulses as for the ^{13}CO, we obtain an estimate of the total gate operation time $T_{\text{gate}} \sim 1.6\times 10^{-3} - 4\times 10^{-5}$ s.

2. Phase gate with the dipole blockade

The dipole blockade mechanism can be used to make the gate operation time equal for all molecules regardless of the relative intermolecular distance. For two molecules in neighboring optical lattice sites with $L=\lambda/2=100$ nm (assuming that molecules are trapped by a lattice field near resonant with the $X\ ^1\Sigma^+ - a\ ^3\Pi$ transition), the shift of the $|\pm\rangle$ states of ^{13}CO due to dipole-dipole interactions is $u=4\mu^2/9L^3\hbar \approx 8.3\times 10^5$ s^{-1} ($\approx$130 kHz).

To perform the phase gate, the pulse sequence described in Sec. III B could be applied. Namely, the π_c pulse first resonantly transfers the control molecule from the $|1\rangle$ state into the $|J=1,F=3/2,M_F=1/2\rangle$ state as shown in Fig. 4(a), followed by the target $2\pi_t$ pulse resonant with the unshifted $|1,J=1\rangle \rightarrow |J=0,J=1\rangle$ transition, where $|1,J\rangle$ denotes the target molecule in the qubit state $|1\rangle$ and the control molecule in the $|J\rangle$ rotational level of the excited electronic state. A final control π_c pulse resonantly deexcites the control molecule back into the $|11\rangle$ state. The resulting phase gate would be given by Eq. (3).

A complication arises, however, since the $J=0 \rightarrow J=0$ transition for the target molecule is forbidden. To circumvent this limitation, the pulse sequence can be modified in the following way. First, an optical π_c pulse excites the control molecule from the $|1\rangle$ state into the $|e'\rangle=|J=1,F=3/2,M_F=1/2\rangle$ sublevel of the $a\ ^3\Pi_0$ state, followed by a microwave π pulse which brings the control molecule into the $|e\rangle=|J=0,F=1/2,M_F=1/2\rangle$ sublevel. Next, a $2\pi_t$ pulse is applied to the target molecule resonant with the unshifted $|1,J=0\rangle - |J=1,J=0\rangle$ transition. It is followed by a second microwave π pulse applied to the control molecule transferring it back into the $|J=1,F=3/2,M_F=1/2\rangle$ state. Finally, the control molecule is deexcited into the $|1\rangle$ qubit state by an optical π_c pulse. The result of this sequence is given by the sixth column of Eq. (6), which shows that the $|10\rangle$ state acquires a minus sign. In order to realize a phase gate, an optical 2π pulse can be applied to the target molecule resonant with the $|11\rangle - |J=1,1\rangle$ transition, which will add a π phase shift to the $|10\rangle$ and $|11\rangle$ states. Finally, only the $|11\rangle$ two-qubit state will have a π phase shift, which implements the phase gate. The resulting gate has the form

$$
\begin{aligned}
&|00\rangle \overset{\pi_c}{\rightarrow} |00\rangle \overset{\pi_{mw}}{\rightarrow} |00\rangle \overset{2\pi_t}{\rightarrow} |00\rangle \overset{\pi_{mw}}{\rightarrow} |00\rangle \overset{\pi_c}{\rightarrow} |00\rangle \overset{2\pi_t}{\rightarrow} |00\rangle,\\
&|01\rangle \overset{\pi_c}{\rightarrow} i|0e'\rangle \overset{\pi_{mw}}{\rightarrow} -|0e\rangle \overset{2\pi_t}{\rightarrow} -|0e\rangle \overset{\pi_{mw}}{\rightarrow} -i|0e'\rangle \overset{\pi_c}{\rightarrow} |01\rangle \overset{2\pi_t}{\rightarrow} |01\rangle,\\
&|10\rangle \overset{\pi_c}{\rightarrow} |10\rangle \overset{\pi_{mw}}{\rightarrow} |10\rangle \overset{2\pi_t}{\rightarrow} -|10\rangle \overset{\pi_{mw}}{\rightarrow} -|10\rangle \overset{\pi_c}{\rightarrow} -|10\rangle \overset{2\pi_t}{\rightarrow} |10\rangle,
\end{aligned}
$$

$$|11\rangle \xrightarrow{\pi_c} i|1e'\rangle \xrightarrow{\pi_{mw}} -|1e\rangle \xrightarrow{2\pi_t} -e^{i\delta\phi}|1e\rangle \xrightarrow{\pi_{mw}} -ie^{i\delta\phi}|1e'\rangle \xrightarrow{\pi_c} e^{i\delta\phi}|10\rangle \xrightarrow{2\pi_t} -e^{i\delta\phi}|10\rangle. \quad (6)$$

Choosing a Rabi frequency $\Omega \sim 10^5$ s^{-1} for both the π_c and $2\pi_t$ pulses (satisfying $\Omega \ll u$) results in the gate time $T_{\text{gate}} = 2\pi/\Omega_\pi + 2\pi/\Omega_{2\pi} \approx 126$ μs. The additional microwave π and optical 2π pulses, applied to the control and target molecules, respectively, can be much shorter, as their Rabi frequencies are not limited by the requirement to be much smaller than the dipole-dipole interaction strength. If the molecules are separated by five lattice periods, for example, the energy shift of the $|\pm\rangle$ states is $u \approx 10^4$ s^{-1} (≈ 1.6 kHz), and the Rabi frequency has to be reduced to fulfill $u \gg \Omega$. If we choose $\Omega \sim 10^3$ s^{-1}, the gate time is $T_{\text{gate}} = 2\pi/\Omega_\pi + 2\pi/\Omega_{2\pi} \approx 12.6$ ms.

The spin-forbidden $X\ ^1\Sigma^+ \rightarrow a\ ^3\Pi$ transition is weakly allowed due to the mixing of the $A\ ^1\Pi_1$ and $a\ ^3\Pi_1$ states by spin-orbit interaction and rotational mixing between the $a\ ^3\Pi_1$ and $a\ ^3\Pi_0$ states [33]. The lifetime of the $J=1$ rotational level of the $a\ ^3\Pi_0$ state is 0.5 s [34], giving the effective transition dipole moment of the optical transition $\mu_{\text{ind}} \sim 2 \times 10^{-4}$ D. The Rabi frequency of the π_c and $2\pi_t$ pulses ($\Omega_\pi = \Omega_{2\pi} = 10^5$ s^{-1}), transferring population to the $a\ ^3\Pi$ state, corresponds to the electric field amplitude of the pulses $\mathcal{E} \sim 3 \times 10^2$ V/cm, with the intensity of the laser pulses $I = c\mathcal{E}^2/4\pi \sim 250$ W/cm^2.

In the case of $^{13}C^{17}O$, the dipole-dipole interaction strength is $u = 3.6 \times 10^5$ s^{-1} for an intermolecular separation $L = 100$ nm, so that choosing $\Omega \sim 4 \times 10^4$ s^{-1} for both π_c and $2\pi_t$ pulses, we obtain $T_{\text{gate}} = 2\pi/\Omega_\pi + 2\pi/\Omega_{2\pi} \sim 300$ μs. For a separation of five lattice periods, the interaction strength reduces to $u \sim 2 \times 10^3$ s^{-1}, and taking $\Omega \sim 2 \times 10^2$ s^{-1} we obtain the phase gate time $T_{\text{gate}} \sim 50$ ms.

The lifetime of the $v=0$, $J=1$ state of $a\ ^3\Pi_0$ is ~ 0.5 s and of the $v=0$, $J=0$ state is virtually infinite; with phase gate operation times of ~ 100 μs-1 ms, the decay of these states during the gate operation will be negligible. Another candidate for the direct phase gate is the NF molecule, which has a small dipole moment $\mu \approx 0.075D$ in the ground electronic $X\ ^1\Sigma^-$ state and $\mu \approx 0.75D$ in the excited metastable $b\ ^1\Sigma^+$ state [35]. The NF molecule is paramagnetic and therefore can be buffer-gas cooled and magnetically trapped just as has been demonstrated for the NH ($X^3\Sigma^-$) molecule [36]. Alternatively, NF molecules in high-dipole moment metastable states $b\ ^1\Sigma^+$ or $a\ ^1\Delta$ can be Stark-decelerated and optically transferred using the stimulated Raman adiabatic passage technique to the ground $X\ ^3\Sigma^-$ state, amenable for magnetic trapping [37].

V. DECOHERENCE MECHANISMS

We consider here the most relevant decoherence mechanisms for our proposed scheme.

Storage and switching state decoherence. In the proposed scheme, qubits are stored in hyperfine sublevels of the ground rovibrational electronic state, which makes them insensitive (at least in first order) to local fluctuations of dc and ac electric fields. The hyperfine sublevels are more sensitive to magnetic field fluctuations, which should be minimized on a time scale of a second, relevant to the lifetime of a molecule in an optical lattice. With nuclear Zeeman splitting scaling as $\sim$ kHz/G, magnetic field fluctuations need to be below a mG. Magnetic-field insensitive $M=0$ hyperfine sublevels can also be chosen as qubit storage states to minimize the related decoherence. The states used to switch on the dipole-dipole interaction have to be long-lived to minimize decoherence from spontaneous emission. With predicted gate operation times of ~ 100 μs and metastable excited state lifetimes of several hundred ms, the decoherence due to spontaneous emission will be small.

Interaction of molecules in the large dipole moment states will give rise to mechanical forces between molecules, leading to motional decoherence. Excitation to the large dipole moment states have, therefore, to be adiabatic. In the direct scheme with the dipole blockade mechanism, molecules are actually never transferred to the large dipole moment states simultaneously, and motional decoherence is minimized. Using deep optical lattices will prevent excitation of higher energy translational states due to optical π and 2π pulses. In the schemes with the CO molecule, the pulses are adiabatic, i.e., much longer (100 μs) than the translational oscillation period (1 μs), and motional excitation will be minimized.

Optical lattice related decoherence. Lifetimes of ultracold molecules in a far-detuned optical lattice of ≈ 1 s have been obtained by minimizing the scattering of lattice photons [38]. Given that the lifetime of a nuclear spin state of a single molecule, isolated from the environment, can be as long as hours, the lifetime of a molecule in a lattice will be the major decoherence mechanism. Excitation of higher energy translational states will result in unwanted decoherence from spatial dependence of the optical π and 2π pulse Rabi frequencies, as analyzed below. It is therefore desirable to load molecules into the translational ground state of the lattice potential.

Decoherence from optical π and 2π pulses. Finite width of the translational ground state of a molecule in a lattice potential also results in a spatially varying Rabi frequency of optical π and 2π pulses experienced by the molecule. As was shown in Sec. III, the ground state width a is related to the wavelength of the trapping laser as $a = \lambda/2\pi(2\eta)^{-1/4} \approx (0.05-0.08)\lambda$ for $\eta = 10-50$. We can roughly estimate the error due to the deviation of the Rabi frequency from the average Rabi frequency $\langle\Omega\rangle = \int \Omega \exp(-r^2/a^2) d^3\vec{r}/(\sqrt{\pi}a)^3$. For a laser beam with a Gaussian profile $\Omega = \Omega_0 \exp(-r^2/2\sigma^2)$, where σ is the half width of the laser beam spatial intensity profile, the averaged Rabi frequency is $\langle\Omega\rangle = \Omega_0/(1+a^2/2\sigma^2)^{3/2}$. From this expression, one can see that to minimize the error due to spatial variation of the area of the optical pulses, a small ratio a/σ is required. It means that laser beams with transverse width $\sigma \gg a$ are necessary. If we assume for an estimate that a laser beam is focused into $\sigma = L = \lambda/2$, equal to the lattice period, we have $a^2/\sigma^2 \sim 0.01$. The average Rabi frequency can then be approximated as $\langle\Omega\rangle \approx \Omega_0(1-3a^2/4\sigma^2)$, giving an estimate of the phase error $\sim 3a^2/4\sigma^2$ during the pulse. Thus the error can be kept below 1% by using laser beams focused down to $\lambda/2$, equal to the separation of molecules in neighboring lattice sites. Tighter

focusing though is needed to avoid excitation of molecules in neighboring sites. One solution is to use a lattice laser wavelength longer than the optical transition wavelength, at the expense of a reduced dipole-dipole interaction strength. Another solution is to utilize the recently proposed technique [39] based on electromagnetically induced transparency, which pumps neighboring molecules into a dark state which does not interact with optical pulses. If one does not use these techniques there will be additional decoherence due to undesirable excitation of molecules in neighboring lattice sites.

In both phase gate implementations, with and without the dipole blockade, the gate operation time is of the order of several hundred μs. For the phase gate without the blockade, the gate time is approximately two-three times smaller compared to the case when the blockade is used. With overall coherence times of the order of 1 s, the maximal number of operations, which can in principle be performed with our scheme, is $\sim 10^4$.

VI. CONCLUSIONS

The analysis of quantum computation proposals with polar molecules trapped in an optical lattice allows one to define a set of requirements for a molecular system optimizing its performance in terms of a quantum gate time, number of operations, coherence time, gate error, and experimental simplicity. A scheme studied in detail in the present work utilizes switchable dipole-dipole interaction between molecules, which can be used to implement a universal two-qubit gate such as a phase gate. It was demonstrated that the proposed scheme to create a phase gate using polar molecules satisfies the set of requirements presented in Sec. II, and is experimentally feasible with current technologies. For the scheme discussed here, molecules with properties similar to CO and NF are suitable. Analysis of decoherence mechanisms present in the system has shown that the phase error per gate can be kept below a threshold value (set at 1% in this work).

In order to make the gate operation insensitive to the relative distance between the molecules, the dipole blockade mechanism has been proposed. Our phase gate can be implemented in the electric field free configuration which makes it highly robust for decoherence related to dipole-dipole interaction. An analysis of decoherence sources shows that the major one will most probably be the loss of molecules from the lattice due to scattering of lattice photons. With the corresponding coherence lifetimes of ~ 1 s, several thousand gate operations are expected to be possible. Finally, the analysis demonstrates that the use of polar molecules in optical lattices is a viable platform for quantum computing, comparing well with neutral atoms in lattices and trapped ions.

ACKNOWLEDGMENTS

The authors gratefully acknowledge financial support from ARO and NSF.

APPENDIX: CALCULATION OF THE PHASE

The phase given by Eq. (1) can be calculated in the first order of perturbation theory. Assuming that the translational ground state wave function width a is much less than the separation between molecules, molecular positions can be written as $\boldsymbol{r}_{1,2}=\boldsymbol{R}_{1,2}+\Delta\boldsymbol{r}_{1,2}$, where $\boldsymbol{R}_{1,2}$ is the position of the minimum of a lattice potential and $\Delta\boldsymbol{r}_{1,2}$ is the deviation of a molecule from that position. We also introduce the vector $\boldsymbol{L}=\boldsymbol{R}_2-\boldsymbol{R}_1$ connecting the potential minima occupied by molecules 1 and 2, as shown in Fig. 2(a). A Taylor expansion can be made in the vicinity of the minima positions

$$\frac{1}{|\boldsymbol{r}_2-\boldsymbol{r}_1|^3}\approx\frac{1}{|\boldsymbol{L}|^3}\left(1-\frac{3(\Delta\boldsymbol{r}_2-\Delta\boldsymbol{r}_1)\cdot\boldsymbol{L}}{\boldsymbol{L}^2}+\frac{6(\Delta\boldsymbol{r}_2-\Delta\boldsymbol{r}_1)^2}{\boldsymbol{L}^2}\right), \tag{A1}$$

$$\frac{1}{|\boldsymbol{r}_2-\boldsymbol{r}_1|^5}\approx\frac{1}{|\boldsymbol{L}|^5}\left(1-\frac{5(\Delta\boldsymbol{r}_2-\Delta\boldsymbol{r}_1)\cdot\boldsymbol{L}}{\boldsymbol{L}^2}+\frac{15(\Delta\boldsymbol{r}_2-\Delta\boldsymbol{r}_1)^2}{\boldsymbol{L}^2}\right). \tag{A2}$$

We keep terms up to second order in $\Delta\boldsymbol{r}_{1,2}$ since higher order terms will result in much smaller error.

The matrix element (1) can now be calculated using a translational ground state wave function of a 3D isotropic harmonic potential $\Psi_g=\exp[-(\Delta\boldsymbol{r})^2/2a^2]/(\sqrt{\pi}a)^{3/2}$, where a is the width of the wave function. The wave function is symmetric, so that terms linear in $\Delta\boldsymbol{r}_{1,2}$ will give zero after averaging. Only $(\Delta\boldsymbol{r}_{1,2})^2$, $(\Delta\boldsymbol{r}_{i1,2})^2$ $(i=x,y,z)$ terms will not average to zero with the corresponding matrix elements $\langle g_1g_2|(\Delta\boldsymbol{r}_1)^2+(\Delta\boldsymbol{r}_2)^2|g_1g_2\rangle=3a^2$, $\langle g_1g_2|(\Delta\boldsymbol{r}_{i1})^2+(\Delta\boldsymbol{r}_i)^2|g_1g_2\rangle=a^2$, respectively.

The term $\hat{\boldsymbol{\mu}}_1\cdot\hat{\boldsymbol{\mu}}_2/|\boldsymbol{R}|^3$ will thus give after averaging

$$\langle\Psi_{1,2};g_1g_2|\frac{\hat{\boldsymbol{\mu}}_1\cdot\hat{\boldsymbol{\mu}}_2}{|\boldsymbol{R}|^3}|\Psi_{1,2};g_1g_2\rangle = \frac{\boldsymbol{\mu}_1\cdot\boldsymbol{\mu}_2}{|\boldsymbol{L}|^3}\left[1+\frac{18a^2}{|\boldsymbol{L}|^2}+O\left(\frac{a^4}{|\boldsymbol{L}|^4}\right)\right]. \tag{A3}$$

The term $(\hat{\boldsymbol{\mu}}_1\cdot\boldsymbol{R})(\hat{\boldsymbol{\mu}}_2\cdot\boldsymbol{R})/|\boldsymbol{R}|^5$ can be written as a sum of four terms

$$\begin{aligned}\frac{(\hat{\boldsymbol{\mu}}_1\cdot\boldsymbol{R})(\hat{\boldsymbol{\mu}}_2\cdot\boldsymbol{R})}{|\boldsymbol{R}|^5} &= \frac{(\hat{\boldsymbol{\mu}}_1\cdot\boldsymbol{L})(\hat{\boldsymbol{\mu}}_2\cdot\boldsymbol{L})}{|\boldsymbol{R}|^5} \\ &+\frac{(\hat{\boldsymbol{\mu}}_1\cdot\boldsymbol{L})(\hat{\boldsymbol{\mu}}_2\cdot(\Delta\boldsymbol{r}_2-\Delta\boldsymbol{r}_1))}{|\boldsymbol{R}|^5} \\ &+\frac{(\hat{\boldsymbol{\mu}}_1\cdot(\Delta\boldsymbol{r}_2-\Delta\boldsymbol{r}_1))(\hat{\boldsymbol{\mu}}_2\cdot\boldsymbol{L})}{|\boldsymbol{R}|^5} \\ &+\frac{(\hat{\boldsymbol{\mu}}_1\cdot(\Delta\boldsymbol{r}_2-\Delta\boldsymbol{r}_1))(\hat{\boldsymbol{\mu}}_2\cdot(\Delta\boldsymbol{r}_2-\Delta\boldsymbol{r}_1))}{|\boldsymbol{R}|^5}.\end{aligned} \tag{A4}$$

After averaging, the first term in Eq. (A4) is given by

$$\frac{(\boldsymbol{\mu}_1\cdot\boldsymbol{L})(\boldsymbol{\mu}_2\cdot\boldsymbol{L})}{|\boldsymbol{L}|^5}\left[1+\frac{45a^2}{|\boldsymbol{L}|^2}+O\left(\frac{a^4}{|\boldsymbol{L}|^4}\right)\right].$$

In the second term of Eq. (A4), taking into account the expansion (A2), only the term

$$-\frac{5(\hat{\boldsymbol{\mu}}_1\cdot\boldsymbol{L})[\hat{\boldsymbol{\mu}}_2\cdot(\Delta\boldsymbol{r}_2-\Delta\boldsymbol{r}_1)][\boldsymbol{L}\cdot(\Delta\boldsymbol{r}_2-\Delta\boldsymbol{r}_1)]}{|\boldsymbol{L}|^7}$$

has to be kept, since all other terms are higher order in a.

In this expression one has to average a sum

$$\sum_{i,j=x,y,z}\hat{\boldsymbol{\mu}}_{2i}(\Delta\boldsymbol{r}_{2i}-\Delta\boldsymbol{r}_{1i})(\boldsymbol{r}^e_{2j}-\boldsymbol{r}^e_{1j})(\Delta\boldsymbol{r}_{2j}-\Delta\boldsymbol{r}_{1j}), \quad \text{(A5)}$$

where i,j denote x,y,z projections of the vectors. Products of the type $\Delta\boldsymbol{r}_{2i}\Delta\boldsymbol{r}_{1j}$, and $\Delta\boldsymbol{r}_{2i}\Delta\boldsymbol{r}_{2j}$, $\Delta\boldsymbol{r}_{1i}\Delta\boldsymbol{r}_{1j}$ with $i\neq j$ will give zero after averaging. Only terms $(\Delta\boldsymbol{r}_{2i})^2$, $(\Delta\boldsymbol{r}_{1i})^2$ will have a nonzero average given by $\langle g_1g_2|(\Delta\boldsymbol{r}_{2i})^2|g_1g_2\rangle=\langle g_1g_2|(\Delta\boldsymbol{r}_{1i})^2|g_1g_2\rangle=a^2/2$. The result of the averaging of Eq. (A5) is $a^2(\boldsymbol{\mu}_2\cdot\boldsymbol{L})$. The contribution from the second term in Eq. (A4) is therefore

$$-\frac{5a^2(\boldsymbol{\mu}_1\cdot\boldsymbol{L})(\boldsymbol{\mu}_2\cdot\boldsymbol{L})}{|\boldsymbol{L}|^7}. \quad \text{(A6)}$$

Averaging of the third term in Eq. (A4) gives the same result as in Eq. (A6). Repeating the same steps the fourth term in Eq. (A4) gives $a^2(\boldsymbol{\mu}_1\cdot\boldsymbol{\mu}_2)/|\boldsymbol{L}|^5$.

Finally, the average of Eq. (A4) is given by the expression

$$\frac{(\boldsymbol{\mu}_1\cdot\boldsymbol{L})(\boldsymbol{\mu}_2\cdot\boldsymbol{L})}{|\boldsymbol{L}|^5}\left[1+\frac{35a^2}{|\boldsymbol{L}|^2}+O\left(\frac{a^4}{|\boldsymbol{L}|^4}\right)\right]+\frac{a^2(\boldsymbol{\mu}_1\cdot\boldsymbol{\mu}_2)}{|\boldsymbol{L}|^5}\left[1+O\left(\frac{a^2}{|\boldsymbol{L}|^2}\right)\right]. \quad \text{(A7)}$$

Adding the expressions (A3) and (A7) one obtains Eq. (2).

The validity of the phase calculation in the first order of perturbation theory can now be analyzed. Terms neglected in Eq. (1) are of the order of $|\langle a_0|\hat{V}_{\text{dip-dip}}|a_i\rangle|^2/(E_i-E_0)$, where $|a_0\rangle=|\Psi_{1,2};g_1g_2\rangle$ and $|a_1\rangle=|\tilde{\Psi}_{1,2};n_1n_2\rangle$; $|\tilde{\Psi}_{1,2}\rangle$ are higher-energy internal (e.g., rotational) states coupled to $|\Psi_{1,2}\rangle$ by the dipole-dipole interaction, $|n_1\rangle$, $|n_2\rangle$ are higher-energy translational states of a lattice potential. The latter are the closest in energy to $|a_0\rangle$, separated by a harmonic potential oscillation frequency, which is in the range $\omega\sim 100$ kHz-1 MHz for deep optical lattices. A contribution from the first excited translational state to the phase (1) will be $\sim a^2|\langle a_0|\hat{V}_{\text{dip-dip}}|a_0\rangle|^2/[L^2(E_i-E_0)]\sim 0.01|\langle a_0|\hat{V}_{\text{dip-dip}}|a_0\rangle|^2/(E_i-E_0)$. The dipole-dipole interaction strength $|\langle a_0|\hat{V}_{\text{dip-dip}}|a_0\rangle|\sim 100$ kHz for molecules with a permanent dipole moment of $\sim 1D$ and intermolecular distance 100–500 nm, will result in the second order contribution to the phase $\sim 0.01|\langle a_0|\hat{V}_{\text{dip-dip}}|a_0\rangle|$. Neglecting this contribution gives a phase error of 1%, which is acceptable in our analysis, and therefore validates the first order approximation given by Eq. (1).

[1] M. A. Nielsen and I. L. Chuang, *Quantum Computation and Quantum Information* (Cambridge University Press, Cambridge, 2000).

[2] *Quantum Communications and Cryptography*, edited by A. V. Sergienko (Taylor & Francis, Boca Raton, FL, 2006).

[3] D. Jaksch, Contemp. Phys. **45**, 367 (2004).

[4] J. I. Cirac and P. Zoller, Nature (London) **404**, 579 (2000); D. Kielpinski, C. Monroe, and D. J. Wineland, *ibid.* **417**, 709 (2002).

[5] A. Rauschenbeutel, G. Nogues, S. Osnaghi, P. Bertet, M. Brune, J. M. Raimond, and S. Haroche, Science **288**, 2024 (2000); J. M. Raimond, M. Brune, and S. Haroche, Rev. Mod. Phys. **73**, 565 (2001).

[6] L. M. K. Vandersypen and I. L. Chuang, Rev. Mod. Phys. **76**, 1037 (2005).

[7] B. E. Kane, Nature (London) **393**, 133 (1998); D. Loss and D. P. DiVincenzo, Phys. Rev. A **57**, 120 (1998); Y. Makhlin, G. Schon, and A. Shnirman, Rev. Mod. Phys. **73**, 357 (2001).

[8] D. DeMille, Phys. Rev. Lett. **88**, 067901 (2002).

[9] C. Lee and E. A. Ostrovskaya, Phys. Rev. A **72**, 062321 (2005).

[10] S. Kotochigova, E. Tiesinga, Phys. Rev. A **73**, 041405(R) (2006).

[11] A. André, D. DeMille, J. M. Doyle, M. D. Lukin, S. E. Maxwell, P. Rabl, R. J. Schoelkopf, and P. Zoller, Nat. Phys. **2**, 636 (2006).

[12] P. Rabl, D. DeMille, J. M. Doyle, M. D. Lukin, R. J. Schoelkopf, and P. Zoller, Phys. Rev. Lett. **97**, 033003 (2006); P. Rabl and P. Zoller, Phys. Rev. A **76**, 042308 (2007).

[13] A. Micheli, G. Pupillo, H. P. Büchler, and P. Zoller, Phys. Rev. A **76**, 043604 (2007).

[14] S. Yelin, K. Kirby, R. Côté, Phys. Rev. A **74**, 050301(R) (2006).

[15] E. Charron, P. Milman, A. Keller, and O. Atabek, Phys. Rev. A **75**, 033414 (2007).

[16] *Spectroscopy of Matrix Isolated Species*, edited by R. J. H. Clark and R. E. Hester (Wiley, Chichester, England, 1989).

[17] J. Doyle, B. Friedrich, R. V. Krems, and F. Masnou-Seeuws, Eur. Phys. J. D **31**, 149 (2004), and references therein.

[18] J. J. Longdell, M. J. Sellars, and N. B. Manson, Phys. Rev. Lett. **93**, 130503 (2004).

[19] D. Leibfried, B. DeMarco, V. Meyer, D. Lucas, M. Barrett, J. Britton, W. M. Itano, B. Jelenkovic, C. Langer, T. Rosenband, and D. J. Wineland, Nature (London) **422**, 412 (2003); A. M. Childs, I. L. Chuang, and D. W. Leung, Phys. Rev. A **64**, 012314 (2001).

[20] E. Knill, Nature (London) **434**, 39 (2005).

[21] D. Jaksch, J. I. Cirac, P. Zoller, S. L. Rolston, R. Côté, and M. D. Lukin, Phys. Rev. Lett. **85**, 2208 (2000).

[22] D. Tong, S. M. Farooqi, J. Stanojevic, S. Krishnan, Y. P. Zhang, R. Côté, E. E. Eyler, and P. L. Gould, Phys. Rev. Lett. **93**, 063001 (2004); K. Singer, M. Reetz-Lamour, T. Amthor, L. G. Marcassa, and M. Weidemuller, *ibid.* **93**, 163001 (2004); R. Heidemann, U. Raitzsch, V. Bendkowsky, B. Butscher, R. Low, L. Santos, and T. Pfau, *ibid.* **99**, 163601 (2007).

[23] M. Fleischhauer, A. Imamoglu, and J. P. Marangos, Rev. Mod.

Phys. **77**, 633 (2005).
[24] A. A. Radzig and B. M. Smirnov, *Reference Data on Atoms, Molecules, and Ions* (Springer-Verlag, Berlin, 1985).
[25] H. L. Bethlem and G. Meijer, Int. Rev. Phys. Chem. **22**, 73 (2003).
[26] H. L. Bethlem, G. Berden, and G. Meijer, Phys. Rev. Lett. **83**, 1558 (1999).
[27] G. Dong, W. Lu, and P. F. Barker, Phys. Rev. A **69**, 013409 (2004).
[28] J. van Veldhoven, H. L. Bethlem, and G. Meijer, Phys. Rev. Lett. **94**, 083001 (2005).
[29] T. Takekoshi, B. M. Patterson, and R. J. Knize, Phys. Rev. Lett. **81**, 5105 (1998).
[30] C. Puzzarini, L. Dore, and G. Cazzoli, J. Mol. Spectrosc. **217**, 19 (2003).
[31] G. Herzberg, *Molecular Spectra and Molecular Structure. Spectra of Diatomic Molecules* (Litton Educational Publishing, Campton, NH, 1950).
[32] C. H. Townes and A. L. Schawlow, *Microwave Spectroscopy* (Dover Publications, New York, 1975).
[33] T. C. James, J. Chem. Phys. **55**, 4118 (1971).
[34] T. Sykora and C. R. Vidal, J. Chem. Phys. **110**, 6319 (1999).
[35] S. Kardahakis, J. Pittner, P. Carsky, and A. Mavridis, Int. J. Quantum Chem. **104**, 458 (2005).
[36] W. C. Campbell, E. Tsikata, Hsin-I. Lu, L. D. van Buuren, and J. M. Doyle, Phys. Rev. Lett. **98**, 213001 (2007).
[37] S. Y. T. van de Meerakker, B. G. Sartakov, A. P. Mosk, R. T. Jongma, and G. Meijer, Phys. Rev. A **68**, 032508 (2003).
[38] G. Thalhammer, K. Winkler, F. Lang, S. Schmid, R. Grimm, and J. H. Denschlag, Phys. Rev. Lett. **96**, 050402 (2006).
[39] A. V. Gorshkov, L. Jiang, M. Greiner, P. Zoller, and M. D. Lukin, e-print arXiv:0706.3879.